# Physical Principles of Magnetohydrodynamic Power Generation

Richard J. Rosa

Citation: Physics of Fluids (1958-1988) **4**, 182 (1961); doi: 10.1063/1.1724426
View online: http://dx.doi.org/10.1063/1.1724426
View Table of Contents: http://scitation.aip.org/content/aip/journal/pof1/4/2?ver=pdfcov
Published by the AIP Publishing

# Physical Principles of Magnetohydrodynamic Power Generation

RICHARD J. ROSA
*Avco-Everett Research Laboratory, Everett, Massachusetts*
(Received October 4, 1960)

Some phenomena apt to be of importance in a magnetohydrodynamic power generator are discussed. Particular attention is given to the effects of seeding on gas conductivity and to the Hall effect as it appears in nonuniform gases of finite extent. An experimental 10-kw magnetohydrodynamic generator is described. An arc wind tunnel or "plasma jet" is used as a convenient laboratory "furnace" to heat the working fluid. The generator's performance, including some observed Hall effects, is presented and discussed.

## I. INTRODUCTION

THE conversion of heat to electric power by the use of magnetohydrodynamics is an idea that has been in existence for many years. However, it is only quite recently that the necessary understanding of and facility for handling high-temperature ionized gases has begun to appear. At the present time magnetohydrodynamic power generation is being actively considered for military and space applications, and in particular, for the large-scale generation of commercial power. The reader is referred to references 1 through 5 for general discussions of this field and surveys of the possible applications.

A simple form of magnetohydrodynamic generator is sketched in Fig. 1. It consists of a duct through which the gaseous working fluid flows, coils which produce a magnetic field across the duct, and electrodes at the top and bottom of the duct. These electrodes serve much the same purpose as the brushes in a conventional generator. The gas, by virtue of its motion through the magnetic field, has an electromotive force generated in it which drives a current through it, the electrodes, and the external load. Such a device would be used in a heat cycle, conventional except for the quite high temperatures involved, and would take over the functions of both the turbine and the generator in such a cycle.

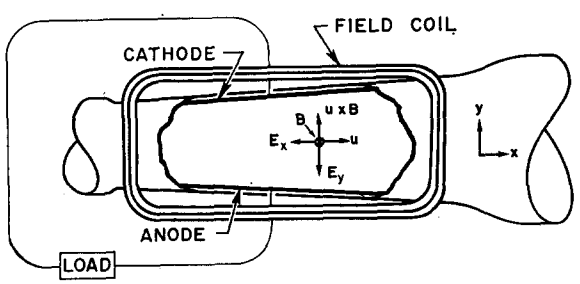


FIG. 1. A linear magnetohydrodynamic generator. Vectors show positive directions for the indicated quantities.

As a branch of magnetohydrodynamics this work meets problems quite different from those encountered in astrophysics and in research on controlled nuclear fusion. The difference between the two is perhaps best summarized by the observation that in this work the magnetic Reynolds number,[6] Rm, tends to be small compared to 1, whereas in fusion research it tends to be much larger than 1. Here $\mathrm{Rm} = \mu_0 \sigma u l$, where $\mu_0$ is the permeability of free space, $\sigma$ and $u$ are the gas conductivity and velocity, and $l$ is a characteristic length.

Since the whole field of magnetohydrodynamics is quite new and since there has been relatively little experimental work in low magnetic Reynolds number magnetohydrodynamics[7] in particular, it is not possible to say just what will prove to be the most important phenomena. In broad terms, low magnetic Reynolds number implies that one is less interested in complex interactions between the fluid and the field, the production of hydromagnetic waves, the occurrence of instabilities, etc. On the other hand, one is more interested in the detailed electrical properties of gases with their dependence

[1] R. J. Rosa, *Advanced Propulsion Systems*, Proceedings of a Symposium held in Los Angeles, California, December 11–13, 1957, edited by M. Alperin, and G. P. Sutton (Pergamon Press, New York, 1959), p. 175.
[2] R. J. Rosa, and A. R. Kantrowitz, Proceedings of the Seminar on Advanced Energy Sources and Conversion Techniques, Pasadena, California, November 3–7, 1958; also, *Direct Conversion of Heat to Electricity*, edited by J. Kaye, and J. A. Welsh, (John Wiley & Sons, Inc., New York, 1960), Chap. 12.
[3] A. Kantrowitz and P. Sporn, Power **103**, 62 (November, 1959).
[4] S. Way, Westinghouse Scientific Paper 6-40509-2-P1, February, 1960.
[5] L. Steg, and G. W. Sutton, Astronautics **5**, 22, 82 (August, 1960).
[6] W. M. Elsasser, Phys. Rev. **95**, 1 (1954).
[7] Frequently called "low-temperature magnetohydrodynamics," since, in general, low (relative) temperature and low magnetic Reynolds number go together.

upon temperature, composition, pressure, and magnetic field strength. In addition, since engineering applications appear more imminent in this area, one finds oneself more seriously concerned with questions of over-all design and the related questions of efficiency, reliability, and economy.

In the following, ionization phenomena in gases and the theory of the operation of magnetohydrodynamic power generators will be reviewed, some basic aspects of their design will be discussed, and some of the important gas phenomena analyzed. Following this, an experimental generator will be described and its operation discussed.

## II. DESIGN CONSIDERATIONS

### A. Gas Conductivity

The distinguishing feature of a magnetohydrodynamic generator as compared to a conventional turbogenerator is that it utilizes an ionized and, hence, electrically conducting gas. Of importance then are the values of conductivity which may be reached and the conditions required to achieve them.

#### *1. Ionization Mechanisms*

There are, broadly speaking, two available ionization mechanisms: first, "thermal" or "equilibrium" ionization obtained simply by heating the gas; and second, "extra-thermal" or "nonequilibrium" ionization such as is obtained in low-pressure gas discharges. Extrathermal or nonequilibrium ionization is more familiar than thermal ionization, since it occurs in such widely used devices as gas rectifiers and fluorescent lights. However, it is, in fact, a considerably more complicated phenomenon. It is not at all clear that it could be used in a way that would yield a net power output.

In thermal ionization, which at present seems most practical, the ionization follows a mass action law as does molecular dissociation. Most common gases such as air, CO, $CO_2$, or the noble gases have a relatively high ionization potential and hence do not ionize thermally until quite high temperatures are reached. However, if a small amount (0.1 to 1%) of some easily ionizable material, such as an alkali metal vapor, is added to the gas,[8] a sufficient degree of ionization can be obtained at temperatures low enough to be withstood by some solid materials, be produced in furnaces, and also conceivably be produced in nuclear fission reactors.

[8] R. J. Rosa, thesis, Cornell University, Ithaca, New York, 1956.

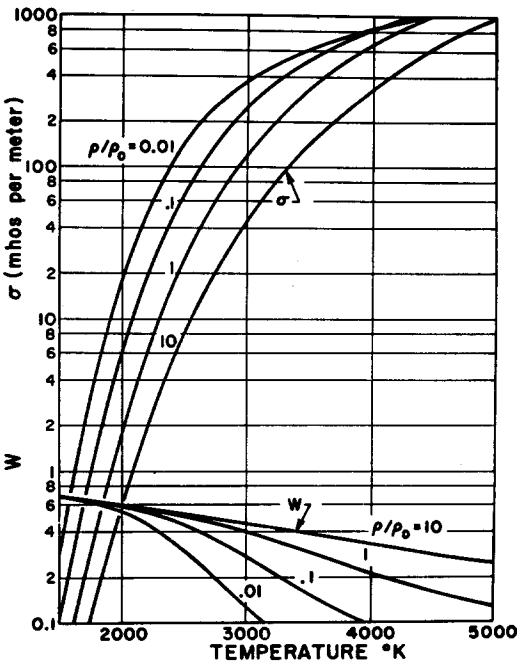


FIG. 2. Conductivity and $\omega\tau$ in argon seeded to 1% with potassium. A Maxwell averaged cross section of $6 \times 10^{-17}$ cm² has been assumed for argon, and a cross section of $3 \times 10^{-14}$ cm² for neutral potassium. The gas density in atmospheres is indicated by $\rho/\rho_0$ and $\omega\tau = WB(\rho/\rho_0)^{-1}$ for $B$ expressed in webers per square meter.

#### *2. Temperature Requirement*

Figure 2 shows calculated values of conductivity for argon plus 1% potassium vapor. It can be seen that argon "seeded" with potassium vapor will have appreciable conductivity at temperatures greater than about 2000°K whereas clean argon becomes essentially nonconducting at about 4000°K.

The value of gas conductivity determines the magnetic field strength and generator size necessary for the production of a given amount of power.

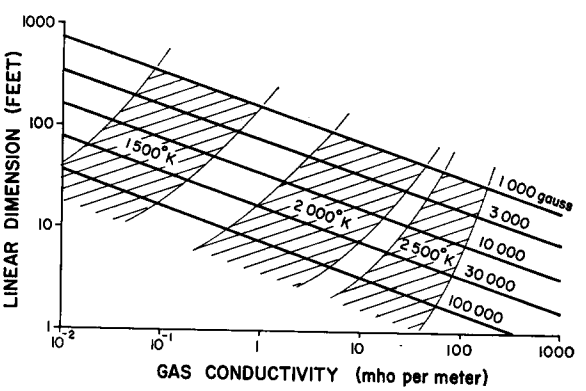


FIG. 3. Approximate size of a 100-Mw magnetohydrodynamic generator as a function of gas conductivity and magnetic field strength. Shaded regions indicated roughly the gas temperatures required.

If the conductivity is too low, so that the generator becomes excessively large, then one expects that the power required to maintain the field, heat transfer and other losses, and also cost and weight will become excessive. Figure 3 shows a plot of the dimensions of a 100 000 kw generator as a function of field strength and gas conductivity. Also indicated approximately are the temperatures required to obtain these conductivities in seeded gases at thermodynamic equilibrium. With this plot we may get at least a rough idea of the conductivity and temperature that we require. A mean linear dimension of 30 ft is a reasonable estimate for the maximum practical size. Then if we take 10 000 gauss as a practical field strength we are led to the conclusion that gas conductivities at least of the order of 1 mho/m, and, hence, temperatures in the neighborhood of 2000°K are required.

### *3. Optimization of Seed Concentration*

It appears that for getting the maximum conductivity there is an optimum value of seed concentration which for most gases is only 1% or less. The reason for this follows from an examination of the collision cross sections of these atoms and of the conductivity equation.

The electrical conductivity of a gas is given by[9]

$$\sigma = 0.532 \frac{e^2}{(m_e kT)^{\frac{1}{2}}} \frac{n_i}{n_i Q_i + n_s Q_s + n_0 Q_0},$$

where $Q_i$, $Q_s$, $Q_0$ are the cross sections and $n_i$, $n_s$, $n_0$ are the number densities of ions, neutral seed atoms, and neutral gas atoms, respectively (the usually very good assumption has been made here that the ion and electron densities are equal); $e$, $m_e$, $T$ are the electron charge, mass, and temperature; and $k$ is Boltzmann's constant.

For alkali metals vapors it appears that the collision cross section $Q_s$ is very large.[10] For the temperatures and degrees of ionization, we can hope to attain in the near future, $n_i$ will be quite small and proportional to $(n_s)^{\frac{1}{2}}$. Thus, approximately

$$\sigma \propto \frac{n_s}{n_s Q_s + n_0 Q_0}.$$

Maximization of this function occurs for $n_s/n_0 = Q_0/Q_s$. For potassium, $Q \approx 3 \times 10^{-14}$ cm$^2$, while for argon the Maxwell averaged cross section, $Q_0$, is reportedly only $6 \times 10^{-17}$ cm$^2$.[10] Thus, in argon, the maximum conductivity is expected for a seed concentration of only 0.2%. The measurements reported in reference 10 are perhaps open to question in the energy range of interest here ($\leq \frac{1}{2}$ ev). However, recent measurements of conductivity in a seeded detonation wave[11] tend to confirm the earlier work.

### B. Flow Theory; Efficiency

The equations governing the essentially one-dimensional flow in a magnetohydrodynamic generator as sketched in Fig. 1 are

$$\text{energy} \qquad \rho u \frac{d}{dx}\left(\frac{u^2}{2} + C_p T\right) = \mathbf{j}\cdot\mathbf{E} \tag{1a}$$

$$\text{momentum} \qquad \mathbf{x}_1 \rho u\, du/dx + \text{grad}\, P = \mathbf{j}\times\mathbf{B} \tag{2a}$$

$$\text{continuity} \qquad \rho u A = \text{const} \tag{3a}$$

$$\text{Ohm's law} \qquad \mathbf{j} = \sigma(\mathbf{u}\times\mathbf{B} + \mathbf{E}) - (\omega\tau/B)\mathbf{j}\times\mathbf{B}, \tag{4}$$

where $P$, $T$, $\rho$, and $u$ are the gas pressure, temperature, density, and velocity; $C_p$ is the constant pressure heat capacity; $j$ is the current density; $E$ and $B$ are the electric and magnetic field strengths; $A$ is the channel cross section; and $\omega$ and $\tau$ are the cyclotron frequency and the mean free time of an electron in the gas. The symbol $\mathbf{x}_1$ denotes a unit vector in the direction of flow.

These equations can be solved in closed form for some special conditions[8] and for more general conditions may readily be integrated numerically.[12] A simplifying feature of magnetohydrodynamic theory under the conditions of interest here is that the magnetic field strength $B$ can usually, to good approximation, be taken as a given thing, fixed by external conditions, and not influenced appreciably by the current patterns that arise in the gas. On the other hand, it is frequently necessary to allow for both the temperature and pressure dependence of the electrical conductivity $\sigma$.

As in a turbine, the flow velocity through a magnetohydrodynamic generator is more or less a constant, the primary effect being a drop in pressure as the gas forces itself through the successive turbine stages of the former, or the magnetic field of the latter. The assumption of strictly constant velocity is useful in that it greatly simplifies the equations of motion and makes clear the processes

[9] S. C. Lin, E. L. Resler, and A. R. Kantrowitz, J. Appl. Phys. **26**, 96 (1955).

[10] S. C. Brown, *Basic Data of Plasma Physics* (Technology Press of Massachusetts Institute of Technology and John Wiley & Sons Inc., New York, 1959).

[11] S. Basu, D.Sc. thesis, Massachusetts Institute of Technology, 1959.

[12] R. M. Patrick and T. R. Brogan, J. Fluid Mech. **5**, 289 (1959).

occurring in the generator.[13] The equations then are

energy $\rho u\, dh/dx = \mathbf{j}\cdot\mathbf{E}$ (1b)

momentum $dP/dx = j_y B$ (2b)

continuity $\rho A = \text{const},$ (3b)

where $h$ is the gas enthalpy per unit mass. The continuity equation now gives the area increase which must be provided to ensure constant velocity.

The rate at which work is done by the gas in pushing itself through the magnetic field is obtained by multiplying Eq. (2b) by $u$

$$u\, dP/dx = j_y u B.$$

The rate at which gas enthalpy is extracted as electrical energy is given by Eq. (1b). Dividing the latter by the former gives (assuming $j_x = j_z = 0$)

$$\eta_e = \frac{\rho u\, dh/dx}{u\, dp/dx} = \rho \frac{dh}{dp} = \frac{E}{uB}, \qquad (5)$$

where $\eta_e$ is the "electrical efficiency" of the generator, i.e., the fraction of the electric power generated that is actually delivered to the load, the difference being dissipated in the internal resistance of the generator itself. It is to be noted that in a conventional generator this power lost in the internal impedance is low-grade heat which must be disposed of, and this not without difficulty. On the other hand, in a magnetohydrodynamic generator this is not lost heat since it remains within the working fluid. However, it does show up as an increased pressure drop or a departure from isentropy or reversibility. This can be seen from Eq. (5), which shows that a decrease in $\eta_e$ results in a decrease in enthalpy extracted for a given pressure drop. The electrical efficiency is thus basically of importance only in that it influences the "turbine efficiency"[14] of the generator. Under the assumption of constant velocity and specific heat, one finds that the real pressure ratio across the generator as compared to the ideal will be given by

$$\frac{P_i/P_f(\text{real})}{P_i/P_f(\text{isentropic})} = \left(\frac{h_i}{h_f}\right)^{\gamma(1-\eta_e)/(\gamma-1)\eta_e},$$

where $h_i$ and $P_i$ are the enthalpy and static pressure at the entrance to the generator, and $h_f$ and $P_f$ are the same quantities at the exit. If this were the only source of pressure loss, the turbine efficiency would be

$$\eta_t = \frac{1 - (P_f/P_i)^{\eta_e(\gamma-1)/\gamma}}{1 - (P_f/P_i)^{(\gamma-1)/\gamma}}.$$

A formula for generator length $L$ can be obtained by integrating Eq. (2b) using Eq. (4) for $j$ and Eq. (5) for $E$. Assuming that $\sigma$, $u$, $\eta_e$, and $B$ are constant, and neglecting for the moment the term in Eq. (4) involving $\omega\tau$, one obtains

$$L = \frac{P_i}{(1-\eta_e)\sigma u B^2}\left[1 - \left(\frac{h_f}{h_i}\right)^{\gamma/(\gamma-1)\eta_e}\right]. \qquad (6)$$

This shows clearly the way length varies with the parameters at one's disposal and so is useful in spite of the several assumptions made in its derivation.

### 1. Eddy Current Losses

Another pressure loss peculiar to a magnetohydrodynamic generator is that due to circulating eddy currents. In a magnetohydrodynamic device the moving conductor is a three-dimensional continuum rather than a bundle of essentially one-dimensional wires. Therefore, eddy currents may occur whenever there is a rapid space variation in electric or magnetic field strength or in gas velocity. For the type of generator in Fig. 1, such variations can be largely avoided except at the entrance and exit. These entering and leaving losses have been analyzed and calculated by Fishman[15] and by Sutton.[16] Under typical conditions it appears that they will be roughly 10% of the entrance stagnation pressure. This is not too serious in a typical power cycle. Moreover, in some cases, it should be practical to put vanes in the entrance nozzle and diffuser to block the eddy current circulation.

### 2. Aerodynamic Losses

As in a conventional turbine, viscous drag and diffuser losses will also occur. However, a magnetohydrodynamic generator has the possibility of being aerodynamically much cleaner, hence such losses may be relatively small.

### 3. Electrode Losses

The electrodes will have a space charge sheath and potential drop associated with them much as in a conventional arc-type gas discharge. The con-

[13] It is shown in Sec. IID that in practice one would probably design more for constant Mach number. However, the difference for present purposes is not great.

[14] Turbine efficiency $=(h_i - h_f)$ (actual)$/(h_i - h_f)$ (isentropic), where $h_i$ is the initial enthalpy and $h_i$ is the final enthalpy obtained for the same pressure drop in either case.

[15] F. Fishman, Avco-Everett Research Laboratory, Research Rept. 78, June, 1959.

[16] G. W. Sutton, General Electric Company Rept. No. TISR595D431, July, 1959.

ditions which will exist in a magnetohydrodynamic generator differ considerably from those under which gas discharges have been studied in the past. However, it has been found experimentally that at least for argon on tungsten the drop is essentially the same (about 8 v) in the generator as in a conventional arc.[17] The percent loss due to this drop will be given by the ratio of this drop to the voltage appearing between electrodes. The latter is given by $(\eta_e uBy)$, where $y$ is the distance between electrodes. Typically, $\eta_e uBy$ is of the order of 1000 v [$u = 1000$m/sec, $B = 1$ weber/m$^2$ (10 000 gauss), $y = 1$ m, and $\frac{1}{2} < \eta_e < 1$] so electrode drops should represent a loss of not more than about 1%.

*4. Heat Transfer and Field Coil Losses*

The two remaining sources of loss are heat transfer to the generator walls and joule dissipation in the coils producing the magnetic field. These two losses are to a considerable extent coupled and hence need to be discussed together.

Wall heat transfer is apt to be one of the largest single sources of loss in a magnetohydrodynamic generator. Thus, the necessity for minimizing it will play a large role in generator design. For a linear configuration as discussed in the foregoing, this means, roughly speaking, that one should avoid duct-length-to-diameter ratios greater than about 20 and high aspect ratio cross sections.

The duct length, according to Eq. (6), is inversely proportional to the magnetic field strength squared; hence, to minimize wall heat loss a high field seems desirable. The joule loss per unit coil length will increase as $B^2$, but since the length goes down as $B^2$ the total field loss will remain more or less constant. Therefore, it appears that the higher the field the better. If iron is used the field is, of course, limited to something less than 20 000 gauss. However, for an industrial size generator, with a more or less square duct cross section, it is possible to design air-cooled field coils which should not consume more than a few percent of the power output, and be reasonably economical. For the size and shape of field desired in a full scale device, the benefits of using iron in the magnetic circuit are, in fact, relatively small.

## C. Hall Effects

There is another important factor to be considered in choosing the magnetic field. Ionized gases, like solid conductors, exhibiting Hall effects which are proportional to the magnetic field strength.[18] Gases at field strengths above a certain (density dependent) value exhibit these effects much more strongly than is usual in solids. At sufficiently high ratios of field strength to gas density a phenomenon sometimes called "ion slip" appears.[19] This phenomenon represents a definite limitation. After it has appeared a further increase in field strength results in essentially no increase in generated electromotive forces or in the force exerted upon the gas as a whole. However, long before this ultimate limit is reached, other phenomena associated with the Hall effect and of great importance for generator design will occur. These will be considered here in some detail.

The term involving $(\mathbf{j} \times \mathbf{B})$ in Eq. (4) (Ohm's law) is the one which gives rise to the Hall effect. Its relative magnitude depends upon the magnitude of the quantity, $\omega\tau$. ($\omega\tau = 2\pi \times$ electron-cyclotron frequency times mean free time.) In terms of gas density in atmospheres $(\rho/\rho_0)$ and magnetic field strength $B$

$$\omega\tau = WB/(\rho/\rho_0), \tag{7}$$

where, as shown in Fig. 2, $W$ is a function of the degree of ionization, electron temperature, and also the gas composition. In the linear generator as $\omega\tau$ approaches and exceeds one, an electric field ("Hall field") will appear parallel to the direction of the flow[20]; that is, the gas stream as a whole will try to assume a higher potential near the exit of the generator than it had at the entrance.

The $x$ and $y$ components of Eq. (4) are (see vector diagram, Fig. 1):

$$j_y = \frac{\sigma}{1 + \omega^2\tau^2}\,[uB - E_y + \omega\tau E_x] \tag{8}$$

$$j_x = \frac{\sigma}{1 + \omega^2\tau^2}\,[\omega\tau(uB - E_y) - E_x]. \tag{9}$$

Strictly speaking the absolute magnitude of the conductivity of a gas is always equal to $\sigma$ until $\omega\tau$ becomes so high that ion slip occurs. However, it is useful here to consider the gas as having an "effective" conductivity defined by

$$\sigma_{eff}/\sigma = j_y/\sigma(uB - E_y).$$

[17] H. S. Morton and R. M. Gage, in *Arcs in Inert Atmosphere and Vacuum*, edited by W. E. Kuhn (John Wiley & Sons, Inc., New York, 1956).

[18] L. Spitzer, Jr., *Physics of Fully Ionized Gases* (Interscience Publishers, Inc., New York, 1956).

[19] A. Schlüter, Z. Naturforsch. **5A**, 72 (1950); **6A**, 73 (1951).

[20] In the following it will always be assumed that "Hall current" or "Hall field" is that component parallel to the gas velocity, **u**, and "conduction current" or "conduction field" is that component in the **u** × **B** direction. This definition of terms is open to criticism, but for the class of problems considered here it seems the least ambiguous.

Figure 4, which is a plot of Eq. (8), shows graphically how this "effective" conductivity will vary with $E_x$ for given values of $\omega\tau$. It can be seen that it will be less than the actual conductivity, $\sigma$ unless

$$E_x = \omega\tau(uB - E_y). \tag{10}$$

If one solves Eqs. (8) and (9) for the Hall field one obtains

$$E_x = \left(\frac{1 - j_x/\omega\tau j_y}{1 + \omega\tau j_x/j_y}\right)\omega\tau(uB - E_y). \tag{11}$$

From this equation it appears that $E_x$ can build up to the value given by Eq. (10), but only if no current, $j_x$, is allowed to flow in the $x$ direction; i.e., if the Hall field is prevented in any way from "shorting out." In principle, this can be done in a linear generator if the electrodes are segmented, with each anode-cathode pair feeding a separate external circuit.

Alternatively, one might design a "Hall current" generator in which the $x$ component or Hall current is deliberately allowed to flow and deliver power to an external load. Such a generator might be advantageous under some conditions although it can be shown to be theoretically somewhat less efficient than a plain "conduction current" type machine such as is discussed in this paper.

A segmented output may well be inconvenient in some applications and constitute a limit on the maximum practical value of $\omega\tau$. In addition, there can be some shorting or leakage of Hall current through the boundary layers of the stream. Predicting the magnitude of this effect accurately is difficult since it requires accurate knowledge of profiles for velocity, conductivity, and $\omega\tau$. Calculation of these will require knowledge not only of wall temperature and of temperature and density profiles, but also of possible high impurity or seed concentrations near the walls. However, boundary layer leakage may usually not be too serious since, in most cases, conductivity in the boundary layer is apt to fall off more rapidly than velocity.

A more general limitation on $\omega\tau$ may arise due to the apparent tendency for it to magnify the effects of any inhomogeneities in gas properties or magnetic field strength within the stream. Ideally, these quantities would be uniform across the channel of a magnetohydrodynamic generator. However, in practice, some variation is bound to occur due, for example, to uneven heating in the thermal energy source, boundary layer cooling, or incomplete mixing of the seed. When it does, it appears that a circulation of Hall current, i.e., a Hall induced eddy current, will result partially shorting out the Hall field.

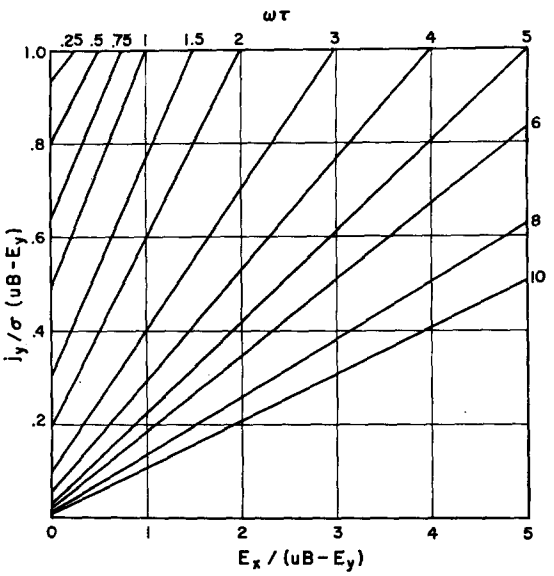


FIG. 4. Relation between "effective conductivity" defined as $\sigma_{eff} = j_y/(uB - E_y)$, and the Hall or axial field $E_x$ for various values of $\omega\tau$.

Variations of $\sigma$ and $\omega\tau$ in the $y$ direction, i.e., in the $(\mathbf{u} \times \mathbf{B})$ direction seem to produce the largest effects. In Appendix I it is shown that for these $y$ variations the equation for $j_y$ keeps the same form as Eq. (8) if appropriate averages across the channel are taken, i.e.,

$$j_y = \left\langle \frac{1 + \omega^2\tau^2}{\sigma} \right\rangle_{av}^{-1} (\langle uB - E_y \rangle_{av} + \langle \omega\tau \rangle_{av} E_x). \tag{12}$$

However, $E_x$ (for $\langle j_x \rangle_{av} = 0$) will no longer be given by Eq. (10) but rather by

$$E_x = \frac{\langle \omega\tau \rangle_{av}}{\langle \sigma \rangle_{av} \langle (1 + \omega^2\tau^2)/\sigma \rangle_{av} - \langle \omega\tau \rangle_{av}^2} \cdot \langle uB - E_y \rangle_{av}. \tag{13}$$

To render this more surveyable, consider an idealized case where the gas stream is divided into two equal parts, one having electrical properties $\sigma_1$ and $\omega\tau_1$, the other with $\sigma_2$, $\omega\tau_2$. If both $\sigma$ and $\omega\tau$ vary, it is quite possible that they will vary in opposite directions. (Note, for example, Fig. 2.) As explained in Appendix I, the two variations will then tend to reinforce rather than cancel one another. The maximum attainable value of $E_x$ is thus shown in Fig. 5 under the assumption that both $\sigma$ and $\omega\tau$ vary by the same factor but in opposite directions, i.e., $\omega\tau_1 > \omega\tau_2$, but $\sigma_2 > \sigma_1$. (Figure 13 in Appendix I shows $E_x$ for variation of either $\omega\tau$ or $\sigma$ alone.) It can be seen that as $\langle \omega\tau \rangle_{av}$ increases, a quite small departure from uniformity can lead to a substantial

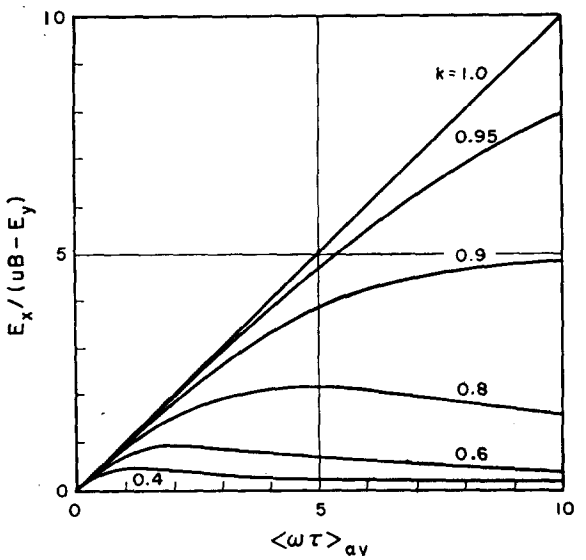


FIG. 5. Reduction in Hall field strength due to eddy currents occurring because of nonuniformity in both conductivity and $\omega\tau$ across the stream. The "degree of uniformity" is given by $k = \sigma_1/\sigma_2 = \omega\tau_2/\omega\tau_1$.

reduction in $E_x$ and hence in "effective" conductivity. It is also interesting to note that for increasing departures from uniformity the value of the Hall field $E_x$ that one will measure becomes quite insensitive to the value of $\omega\tau$ over a considerable range.

### D. Optimum Flow Velocity

The velocity of the gaseous working fluid in a generator and its electrical conductivity are tied together through the gas temperature.

The conductivity will, in general, be an exponential function of temperature at low temperatures. At higher temperatures, as the degree of ionization exceeds about 0.1%, the conductivity becomes proportional to the three-halves power of the temperature. Figure 2 exhibits this general tendency (although the fact that the gas is seeded rather than pure has an effect on the shape).

As the working fluid accelerates into a generator, its temperature, and, hence, its conductivity, drops. Since both high velocity and high conductivity are desirable, the question arises as to what compromise between the two should be chosen.

By the use of Eqs. (1) through (5) one can show that the power output per unit volume of flow is proportional to the produce $(\sigma u^2)$. On the other hand, the amount of gas enthalpy which is extracted per unit length of flow path is proportional to the product $(\sigma u)$. In the design of a specific generator one will probably seek to maximize one or the other of these two products.

For a given stagnation temperature, one can readily calculate the temperature after acceleration and hence the Mach number that will maximize either $\sigma u$ or $\sigma u^2$ in the limit of "high" or "low" degrees of ionization. The results of such a calculation are listed in Table I. In the table, $T_i$ is the

TABLE I. Optimum Mach number.

| Ionization | Optimum $T/T_s$ Low | High | Optimum Mach No. ($\gamma = 1.67$) Low ($T_s/T_i = 0.1$) | High |
|---|---|---|---|---|
| $\sigma u^2$ | $1 - T_s/T_i$ | 0.6 | 0.6 | 1.4 |
| $\sigma u$ | $1 - \frac{1}{2}T_s/T_i$ | 0.75 | 0.4 | 1.0 |

temperature equivalent of the ionization potential of the gas; $T$ is its local temperature; and $T_s$ is its stagnation temperature.

The Mach numbers corresponding to the indicated optimum temperature ratios are also given for a $\gamma = 1.67$ gas and for $T_s/T_i = \frac{1}{10}$. Although supersonic Mach numbers are indicated for some conditions, it is possible that a consideration of other factors such as diffuser losses would rule them out in practice.

### E. Geometric Considerations

Up to now a linear device as sketched in Fig. 1 has been the only one discussed. Numerous geometric variations can be conceived of which operate as Hall or conduction-type devices or possibly as combinations of both.[21] Two of what are probably the most basic variations are sketched in Fig. 6. These are a disk or spiral geometry and a coaxial geometry. In the disk geometry, power must be extracted via the conduction current. Hall currents can circulate freely within it, and if $\omega\tau$ is not small compared to one, a substantial reduction in effective conductivity will result. In contrast to the disk, the coaxial geometry[22] requires that power be extracted via the Hall current, and if $\omega\tau$ is not large compared to one, performance will suffer.

As a Hall generator, the coaxial geometry has the advantage that it does not require the multiplicity of electrodes that the "straight" geometry does. As a conduction generator the disk has the advantage over the straight geometry in that one can place the cathode at the center and avoid the

[21] A generator is defined here as a Hall or conduction-type device depending upon whether the Hall or conduction current is led off via electrodes and passed through the external load.

[22] B. Karlowitz, *et al.* U. S. Patent 2,210,918, 13 August 1940.

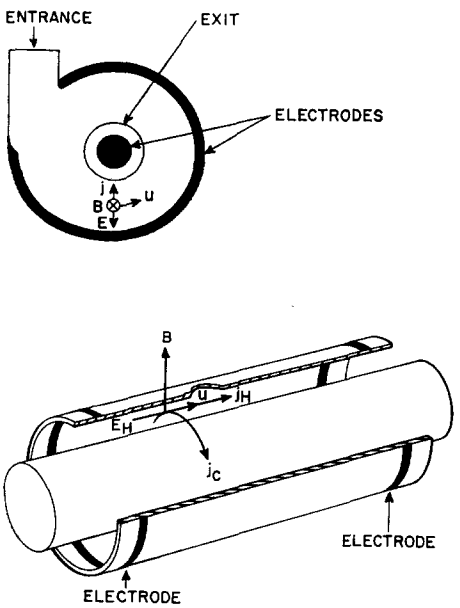


FIG. 6. Disk and coaxial generator geometries. Vectors show positive directions for the indicated quantities.

necessity of providing a distributed source of electron emission.

For a given enclosed volume (and hence approximately for a given design power output), a disk has the least surface area and a coaxial geometry has the most. Hence, a coaxial geometry is worst from the point of view of heat transfer and viscous losses. One can show that a coaxial geometry will have two to four times as much surface area as a straight one, and a straight geometry will have two to four times as much as a disk.

Again, with respect to magnetic field, a little reflection will show that the disk geometry is apt to be the easiest to provide for (i.e., is most economical of iron, copper, and power), and the coaxial geometry is clearly the most difficult.

It can be seen that in the preceding respects the straight geometry occupies a position intermediate between the disk and coaxial geometries. However, at least in the present experimental stage of magnetohydrodynamic generator development the straight geometry has two distinct advantages. First is the ability to operate at any value of $\omega\tau$, including those between "high" and "low" (i.e., between about $\frac{1}{3}$ and 3), and to operate as either a Hall or conduction current device or any mixture thereof. Second is the fact that, when operated as a conduction current generator, a relatively high degree of decoupling exists between upstream and downstream parts of the flow. This permits one to dissect and analyze its performance more easily and to more easily allow for variations in gas properties, principally conductivity and $\omega\tau$, as the gas expands and cools in passing through the device. (Note that in the disk, the coax, and the straight Hall geometries the same current passes through the gas near the entrance to the generator and near the exit; hence, the current density at any point is a strong function of what is going on throughout the device.)

In summary, the straight geometry, while inferior in some respects to the others, seems quite a bit superior to them in flexibility. It remains to be seen whether or not this flexibility (in particular the ability to operate with intermediate values of $\omega\tau$) will be of dominant importance when one is engineering a practical device.

## III. EXPERIMENTAL

### A. Introduction—Description of Apparatus

In this work an "arc wind tunnel"[23] or "plasma jet" was used as the most convenient and flexible laboratory method for heating the working fluid. A photograph of the experimental facility is shown in reference 24 and a schematic diagram is shown in Fig. 7. Its operation is briefly as follows. Argon and powdered potassium carbonate are injected into the arc tunnel at about 3 atm pressure and there mixed and heated to approximately 3000°K. At this temperature the $K_2CO_3$ dissociates and the free potassium partially ionizes making the gas, as a whole, an electrical conductor. The gas then accelerates in a nozzle and passes into a channel between the poles of the magnet. This channel, lined with electrodes, forms a straight generator configuration of the type sketched in Fig. 1. After passing through the generator, the gas discharges into a tank which is ducted to the roof.

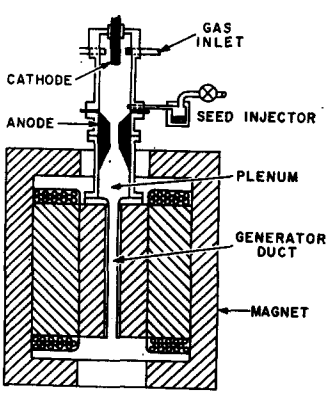


FIG. 7. Schema of the magnetohydrodynamic generator experiment.

[23] T. R. Brogan, American Rocket Society Paper 724-58 (1958).
[24] R. J. Rosa, J. Appl. Phys. 31, 735 (1960).

In planning the scale of this experiment, it was desired that the device do more than just produce an observable amount of power. It seemed that it should simulate a full-scale magnetohydrodynamic generator more or less to the same extent that one turbine stator-rotor stage simulates a full-scale turbine. That is, it should extract a few percent of the gas enthalpy and cause a pressure drop approaching half the stagnation pressure. This requirement was imposed in an effort to ensure that the effects would indeed be clearly observable, and that the device, if it worked, could be a useful first step toward the practical application of magnetohydrodynamics to power generation rather than a mere laboratory curiosity.

In the interests of economy and flexibility neither the arc tunnel nor the generator duct employed water cooling. This, of course, limited the duration of runs. However, operating times of 5 sec were employed with no visible damage. Since steady-state conditions were usually reached within a small fraction of a second, the available safe testing time was more than adequate for the objectives of this study.

The very simple seed injection system used gave an injection rate controllable to within a factor of about 2. A far greater uncertainty is involved in predicting just what fraction of the powder actually mixed with the stream, evaporated into gas, and dissociated, releasing free atomic potassium. However, good conductivity with reasonably good reproducibility was achieved. Measurements of conductivity and of $\omega\tau$ indicated that most of what was injected did in fact get into the stream.

It was found that the system as a whole, arc tunnel plus generator, seemed to work best with a seeding rate of about 1 g of $K_2CO_3$ per 100 g of argon in spite of the fact that the optimum amount of potassium in pure argon should be no more than about two-tenths of 1%.

### B. Conductivity and Electrode Drop Experiments

In the course of this work the electrical conductivity of the gas was measured several times and by two different techniques. During the first runs with the tunnel, a 1- by 10-cm slot-shaped nozzle was used. Pictures were taken of the exhaust to determine uniformity and a series of runs were made exhausting through an insulated channel that had a coil imbedded in one wall. This coil was resonated with a condenser at about 300 kc and the damping of this circuit by the exhaust was measured to determine gas conductivity. Calibration was effected by placing various salt solutions in the channel. During these tests, conductivities of about 60 mhos/m were measured.

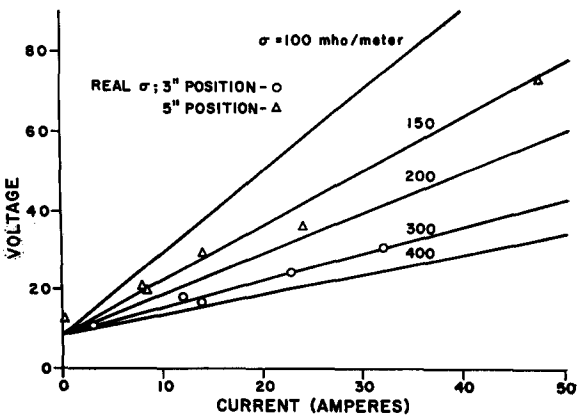


FIG. 8. Gas conductivity and electrode drop measurements in a short 1.3- by 10-cm channel.

Subsequent to these tests, the design of the tunnel was improved and its operating power level increased. Then to determine both electrode drops and gas conductivity, two sets of tungsten rod electrodes were placed in the short sides of a 1.3 × 10-cm channel—one set placed 3 in. and one set 5 in. from the entrance. With no magnetic field present, various voltages were impressed between anodes and cathodes with an external power supply and the resulting current flow during a run was measured. The results are plotted in Fig. 8 for both sets of electrodes.

The slope of a line through the data gives the gas conductivity, and its intercept at zero current indicates the sum of the anode and cathode drops. Although no great accuracy can be claimed for these measurements, they indicate that the electrode drops are quite low (6 to 10 v) corresponding closely with what has been measured in a conventional tungsten arc in argon,[17] this in spite of the very different conditions existing in the two cases. Also indicated is the fact that the gas conductivity (150 to 300 mhos/m) was very good but dropped quite rapidly with distance along the channel.

In order to obtain the best correlation with the power generating runs to be described in the following, a third set of conductivity measurements was made by impressing a voltage across the electrodes of the channel used for these runs. The results are shown in Fig. 9. This channel had a relatively large cross section, and the ratio of arc heater power to mass flow rate was lower than for the previous measurements. Hence, the gas con-

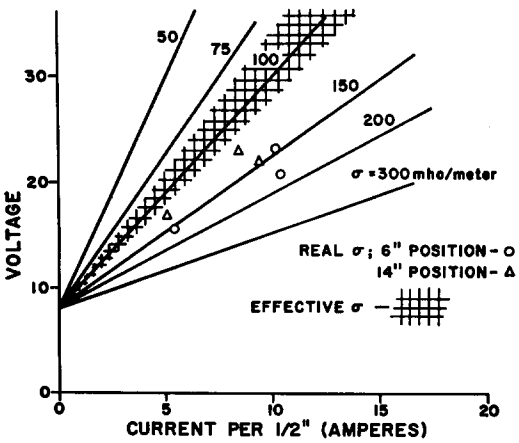


FIG. 9. Gas conductivity measurements in the channel used for the power generation experiments described in the text. The "effective conductivity" as deduced at various points along the channel during the generation runs is indicated by the crosshatched region.

ductivity was somewhat lower, averaging around 150 mhos/m, but dropped much more slowly with distance along the channel.

### C. Power Generation Tests

#### *1. Channel and Electrode Configuration*

The power generation tests to be described were done in the 1- by 3-in. channel sketched in Fig. 10. The channel walls including the blocks holding the electrodes were made of transite. The electrodes were $\frac{1}{16}$-in. diam tungsten rods spaced $\frac{1}{2}$ in. apart in a double row. Each set of four anodes and four cathodes was connected to two load resistors as shown in Fig. 10. Each of the 20 sets of electrodes fed a separate pair of load resistors and hence was electrically isolated from every other set. Thus, output as a function of position down the channel could be studied and each set of electrodes was free to float at a different potential under the influence of Hall effects. In addition, this tended to counteract any tendency for one electrode to "take over" and carry all the current. This tendency, however, seems less in a generator than it would be in the case of several conventional discharges burning in parallel. It was found in practice that all four commonly connected anodes carried approximately the same current. There was a small but consistent difference which could be correlated with the Hall effect and with the direction of the swirl which was given to the gas in the arc chamber, and evidently persisted to at least some extent during mixing and acceleration into the generator.

In the case of the cathodes, this same correlation with Hall effect and swirl direction was noted. However, in this case one cathode would eventually take over almost entirely from the other after 1 or 2 sec of operation. This greater instability of the cathode is what one would expect from experience with conventional discharges.

The cross-sectional area of this channel was roughly constant. No exit diffuser was used, the channel discharging directly to the atmosphere. Static pressure measurements were taken in the upstream plenum chamber and at three points along the channel. From these measurements it appears that the flow acted as though the channel cross section was about 15% smaller at the exit than at the entrance. Boundary layer growth,[25] greater erosion of the channel walls near the entrance, and the projecting electrodes would all tend toward such an effect.

During a run, data were taken by photographing an array of panel meters and pressure gauges at the rate of about 10 frames/sec. Use of a monobath developed at the Avco-Everett Research Laboratory[26] afforded rapid availability of the data.

#### *2. Generator Performance*

Figure 11 shows performance data obtained during a set of six runs all made with the channel described in the foregoing and under as nearly similar conditions as possible, the only intentional variable being the value of load resistance. The data presented are representative in that reproducible results were usually obtained except in some 20% of the runs. Then, for not fully understood reasons the arc tunnel would operate at a higher or lower current

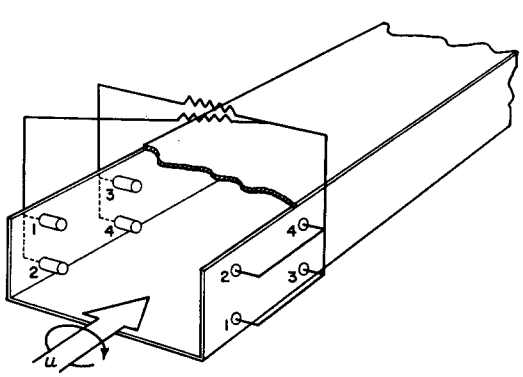


FIG. 10. Electrode and wiring diagram for the power generation experiments described in the text. One set of electrodes is shown. The complete generator consisted of 20 such sets. The small arrow indicates the direction of swirl given to the gas in the arc chamber.

[25] Calculations indicate that fully developed turbulent pipe flow occurred by the time the flow reached the exit.
[26] S. Braunstein (unpublished).

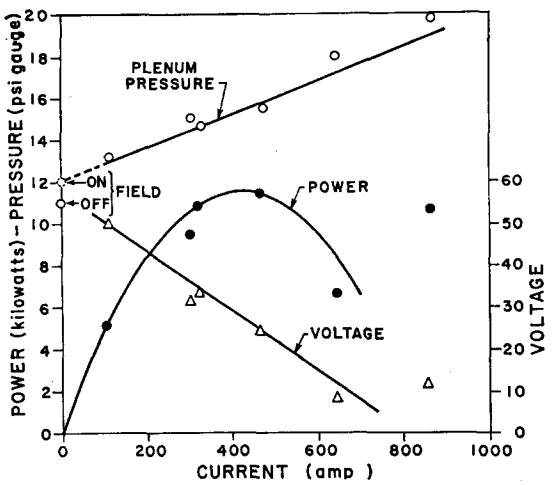


FIG. 11. Upstream plenum pressure, output voltage, and power output as a function of total output current.

than usual. Even in these cases, however, it was possible to correlate the performance of the generator with the performance of the arc tunnel. (It is likely that a large fraction of the fluctuations can be attributed to the seeding system.)

In Fig. 11, total power output, average voltage, and pressure in the upstream plenum chamber are plotted against total current (i.e., sum of currents through each load resistor). The power-output data show the largest scatter[27] because they involve taking the square of measured quantities. The solid lines are a theoretical fit to the experimental points. The data as a whole may be summarized by remarking that they do not differ basically from those one would get out of a test of a turbogenerator as, indeed, in theory they should not.

All runs were made at the same mass flow rate, chosen just high enough so that the exit Mach number was at or near one. If we make the assumption that the exit velocity was the same for all runs, then the upstream plenum pressure should be given simply by

$$P_I = \int_0^L jB\,dx + P_{I=0},$$

which for the field (14 000 gauss) and the channel used reduces to

$$P_I(\text{psi}) = 0.82 \times 10^{-2} I + P_{I=0},$$

where $I$ is the total generator current in amperes. Experimentally a value for $P_{B=0}$ was obtained by turning off the magnet in the middle of one of the runs. If $I$ had instead been reduced to zero by open circuiting all the loads, one would still expect some pressure drop to occur due to circulating eddy currents at the channel entrance and exit. For this device the eddy current drop has been calculated to be about 1 psi. Hence, a semitheoretical open-circuit plenum pressure is plotted in Fig. 11 using for $P_{I=0}$ the value $(P_{B=0} + 1)$. It can be seen that this choice of zero-point pressure does give an appreciably better fit to the other data.

The "theoretical" voltage-current curve was obtained simply by drawing the best line through the data and the theoretical power curve obtained from this by using the known values of load resistance. This analysis admittedly neglects variations in gas velocity and conductivity occurring because of change in load resistance. However, the expected variation, amounting to about 15% at the high-current end of the scale, is less than the scatter in the data.

The slope of the voltage-current line is a function of the "effective" gas conductivity. It is significant that the "effective" conductivity deduced in this way (see Fig. 9) is apparently some 30% less than the measured values. A certain amount of internal shunting of the generator through the boundary layers may have occurred. However, it seems likely that a Hall induced eddy effect, as discussed earlier, plus leakage of Hall current through the boundary layers was at least partly responsible.

### *3. Hall Effects*

During the power generation runs just described, the Hall field, i.e., the voltage gradient parallel to the flow, was measured at five locations along the channel. The ratio of the Hall field $E_x$ to the net electromotive force across the flow $(uB - E_y)$ was found to average about 0.6. This implies an $\omega\tau$ of about 0.6 if no Hall current leakage or Hall eddy effect has occurred. However, since it is likely that both of these effects did occur, one can estimate that $\omega\tau$ during these runs probably had a mean value of a little over one.

Having a measure of both $\omega\tau$ and the conductivity, it is possible to go back and deduce roughly the mean atom-electron collision cross section of the gas. This turns out to be between $3 \times 10^{-16}$ and $6 \times 10^{-16}$ cm$^2$ or over five times the cross section one would expect in pure argon. To get this value one must assume a 1–2% concentration of potassium

[27] It is interesting to note that the point which shows the largest scatter might be explained by the assumption that at a high enough current density electrode drops substantially vanish. However, the author is not aware of any good theoretical or experimental justification for such an assumption other than the fact that very small voltage drops are sometimes exhibited by discharges with externally heated cathodes.

(note Fig. 2) indicating that most of what was injected did, in fact, get vaporized, dissociated, and mixed into the stream.

In an attempt to obtain and study the effects of higher values of $\omega\tau$, a number of generating and conductivity measuring runs were made using reduced seeding rates and arc heater powers. In this way, up to a factor of 3 difference between real and effective conductivity was obtained. This, together with a measured Hall field approximately equal to $(uB - E_y)$, indicates (Fig. 4) that $\omega\tau$ was up to a value of between 3 and 4. These results illustrate that in practice one may want to use a higher seed concentration than that giving the highest real conductivity just in order to avoid Hall effects.

Several interesting runs were also made during which Hall current was deliberately allowed to flow part of the time in the first half of the channel. This was done by connecting an electrode near the entrance to one in the middle through a switch that could be opened and closed during a run. A time history of Hall current, Hall voltage, and output ("conduction") current during one of these runs is shown in Fig. 12. Hall voltage and output current history for points in both the first and second halves of the channel are shown. The marked effect of allowing Hall current to flow is evident. It should be observed that measurements of the change in Hall voltage, Hall current, and conduction current made during these runs, although interesting in themselves, are of limited value for deducing $\omega\tau$.

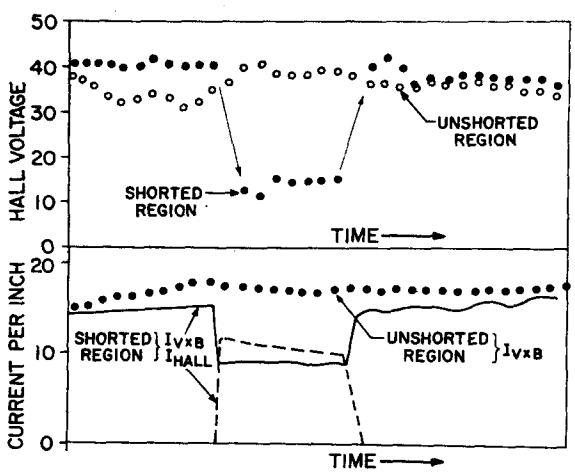


FIG. 12. The effect of deliberately allowing Hall current to flow in the first half of the generator channel. The data indicated by discrete points were obtained from panel meters photographed at the rate of about 10 frames/sec and show overswing and oscillation characteristic of these meters. The lines (solid and dashed) portray data obtained from oscilloscopes.

All these changes, like the absolute value of the Hall field itself, become relatively insensitive to the value of $\omega\tau$ when inhomogeneities (or some other shorting effects) exist. It is estimated that the degree of uniformity as defined in connection with Fig. 5 had the rather low value of 0.5 to 0.6 during these experiments.

In a practical application of magnetohydrodynamic power generation one can probably obtain greater uniformity and smaller boundary effects than were obtained in this arc-heated experiment. For this reason the quantitative results of this series of runs is of limited significance. However, qualitatively they seem to verify our basic theoretical understanding of Hall effects in gases. More important, they underline the need to investigate how these effects work out in practical situations where inhomogeneous gas properties and boundary effects are bound to occur.

## CONCLUSIONS

The experimental work described in the foregoing has shown that, at least qualitatively, our understanding of magnetohydrodynamics, of gas conductivity, electrode performance, and Hall effects is correct. It has demonstrated the basic feasibility of magnetohydrodynamics as a means of power generation. There still exists the very much larger task of obtaining the quantitative data and engineering experience required for the design of a useful long-lived and efficient conversion system.

## ACKNOWLEDGMENT

The author is grateful for the technical assistance of H. Resnick. In addition, he must acknowledge his indebtedness to the prior work of many people, in particular to Dr. A. Kantrowitz and to T. R. Brogan, S. C. Lin, R. M. Patrick, and H. Petschek who, under the direction of Dr. Kantrowitz, laid the foundations for the present work.

This work was partially supported by the Ballistic Missile Division, Air Research and Development Command, U. S. Air Force, under contract.

## APPENDIX A

### Eddy Currents Induced by Inhomogeneities and the Hall Effect

By referring to Fig. 1, if there are variations in the $y$ direction in the values of conductivity and $\omega\tau$, then it is possible for the Hall current to circulate within the stream and adversely effect the performance of a magnetohydrodynamic device. At any

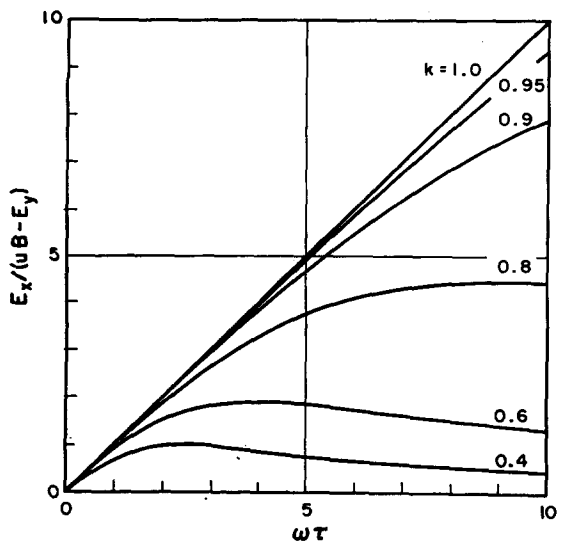


FIG. 13. Reduction in Hall field strength due to non-uniformity in conductivity alone across the stream. The "degree of uniformity" is given by $k = \sigma_1/\sigma_2$. For non-uniformity in $\omega\tau$ alone multiply ordinate by $(k + 1)^2/4k$.

point in the stream the component Eqs. (8) and (9) (Sec. IIC) must be satisfied. Assume $j_y$ and $E_x$ are not functions of $y$ but that $u$, $B$, $E_y$, and $j_x$ can be. Let us integrate Eq. (8) as follows:

$$\frac{j_y}{Y}\int_0^Y \frac{1+\omega^2\tau^2}{\sigma}\,dy = \frac{1}{Y}\int_0^Y (uB - E_y)\,dy + \frac{E_x}{Y}\int_0^Y \omega\tau\,dy,$$

This is by definition [Eq. (12)]

$$j_y = \left\langle \frac{1+\omega^2\tau^2}{\sigma} \right\rangle_{av}^{-1} (\langle uB - E_y\rangle_{av} + \langle\omega\tau\rangle_{av}E_x),$$

which gives $j_y$ in terms of the externally measurable quantities $\langle uB - E_y\rangle_{av}$ and $E_x$ and averages of functions of $\omega\tau$ and $\sigma$.

Elimination of $(uB - E_y)$ between Eqs. (8) and (9) gives the point equation

$$j_x = \omega\tau j_y - \sigma E_x. \tag{A.1}$$

This equation shows that in a generator the Hall current will tend to flow downstream in layers of high $\omega\tau$ or low conductivity and return upstream in layers of low $\omega\tau$ or high conductivity. Thus, the effect will be greatest for variation of $\sigma$ and $\omega\tau$ in opposite directions. It can also be deduced that $y$ variation of $u$ or $B$ will not of itself give rise to eddy currents. Integration of Eq. (A.1) for $j_x$ across the stream under the assumption $\langle j_x\rangle_{av} = 0$ gives

$$j_y = (\langle\sigma\rangle_{av}/\langle\omega\tau\rangle_{av})E_x. \tag{A.2}$$

(It is interesting to note from this the direct proportionality between $j_y$ and $E_x$ under the condition $\langle j_x\rangle_{av} = 0$.) Now eliminating $j_y$ between Eqs. (12) and (A.2) gives the expression for $E_x$ in the presence of inhomogeneities

$$E_x = \frac{\langle\omega\tau\rangle_{av}}{\langle\sigma\rangle_{av}\langle(1+\omega^2\tau^2)/\sigma\rangle_{av} - \langle\omega\tau\rangle_{av}^2}\langle uB - E_y\rangle_{av}. \tag{13}$$

Figure 5 shows this equation graphically for the simplified conditions outlined in Sec. IIC and for variation of both $\omega\tau$ and $\sigma$. Figure 13 shows it for variation of $\sigma$ alone. For variation of $\omega\tau$ alone one may use the values from Fig. 13 multiplied by the factor

$$\frac{E_x\,(\text{variable }\omega\tau)}{E_x\,(\text{variable }\sigma)} = \frac{(k+1)^2}{4k}.$$

Since this factor does not differ appreciably from unity for values of $k > 0.5$, one may, for most purposes, use Fig. 13 directly for either variable $\omega\tau$ or variable $\sigma$.